PHYSICAL REVIEW B **82**, 161412(R) (2010)

Molecular structure of the H_2O wetting layer on Pt(111)

Sebastian Standop,[1,*] Alex Redinger,[1] Markus Morgenstern,[2] Thomas Michely,[1] and Carsten Busse[1]
[1]*II. Physikalisches Institut, Universität zu Köln, 50937 Köln, Germany*
[2]*II. Physikalisches Institut (IIB) und JARA-FIT, RWTH Aachen, 52056 Aachen, Germany*
(Received 2 July 2010; published 19 October 2010)

The molecular structure of the wetting layer of ice on Pt(111) is resolved using scanning tunneling microscopy. Two structures observed previously by diffraction techniques are imaged for coverages at or close to completion of the wetting layer. At 140 K only a $\sqrt{37}\times\sqrt{37}R25.3°$ superstructure can be established while at 130 K also a $\sqrt{39}\times\sqrt{39}R16.1°$ superstructure with slightly higher molecular density is formed. In the temperature range under concern the superstructures reversibly transform into each other by slight changes in coverage through adsorption or desorption. The superstructures exhibit a complex pattern of molecules in different geometries.

DOI: 10.1103/PhysRevB.82.161412 PACS number(s): 68.43.Hn, 68.08.Bc, 68.35.Rh, 68.37.Ef

The wetting layer of H_2O on metal surfaces is one of the most studied systems in surface science,[1] addressed utilizing different experimental and theoretical techniques on various substrates.[2,3] Traditionally, the first adsorbed layer on many hexagonal surfaces of transition metals is rationalized as a single dense-packed ice I_h (0001) plane cut out of the crystal and transferred to the substrate. In a strict interpretation the buckled nature of this plane persists and consequently the ice layer is bound to the metal via an oxygen lone pair of every second molecule whereas one H of every other molecule is pointing upwards (H-up model). However, in the case of Pt(111) there is experimental evidence ruling out that a significant number of free OH groups extend into the vacuum,[4–7] leading to a model where the respective H is positioned between O and Pt (H-down model). A third possibility is that the molecular plane is parallel to the surface, i.e., a flat laying molecule. This is also the energetically preferred geometry for monomers on several metals. As a consequence, for Ru(0001),[8] Cu(110),[9] and Pd(111) (Ref. 10) structures have been observed which maximize the number of such flat lying molecules.

The intuitive structural relation in these systems is a simple commensurate $\sqrt{3}\times\sqrt{3}R30°$ superstructure ($\sqrt{3}$ for short), see Refs. 2 and 3 for examples. However, often the strength of the molecule-metal bond is comparable to the molecule-molecule interaction which leads to high-order commensurate (HOC) superstructures, as for H_2O/Pt(111). He-Atom-scattering[11] and low-energy electron diffraction[5,12] showed a $\sqrt{37}\times\sqrt{37}R25.3°$ superstructure ($\sqrt{37}$ for short) for extended water islands that changes into $\sqrt{39}\times\sqrt{39}R16.1°$ ($\sqrt{39}$ for short) with increasing coverage. The molecular structure, however, remains unsolved. The existing scanning tunneling microscopy (STM) data revealed three phases[13] which could not be reconciled with those found in diffraction.[3] An experimental problem is that the structures are very sensitive and are transformed into the $\sqrt{3}$ by prolonged electron exposure.[5,14] In principle, the structure of the supercell can be calculated using density functional theory (DFT), but for the cell sizes present here, as for an accurate description of hydrogen bonds, this approach is very demanding. Specifically, calculated adsorption energies are often too small to explain wetting.[15,16] On the basis of molecular resolved images of the pure H_2O wetting layer and an analysis of its stability and phase transformations we present here the key elements of the molecular structures of the wetting layer phases.

The experiments were performed in an ultrahigh-vacuum STM system (base pressure $p<1.5\times10^{-11}$ mbar). The sample was prepared by cycles of 5 keV Ar^+ bombardment and flashing (1270 K). The azimuthal sample orientation was calibrated using the close-packed steps bounding large vacancy islands created by sputtering at 650 K. Just before H_2O exposure, the sample was flashed to 730 K to desorb recaptured adsorbates, especially CO. Thoroughly Ar bubbled, ultrapure H_2O was deposited from an Au coated reservoir via a glass tube ending in close proximity to the sample. The dose was calibrated by measuring the pressure in the reservoir of defined volume through a spinning rotor gauge. The typical dose of 0.8 molecules/Pt site ensured a saturated wetting layer. During and till 300 s after adsorption the sample was kept at $T_{ads}\geq130$ K, which allows adsorbate ordering and re-evaporation of excess molecules not part of the wetting layer.[17] To impede subsequent adsorption of impurities, the sample was moved into a cylindrical cold wall (liquid N_2) immediately after dosing and cooled to STM imaging temperatures (20–100 K if not stated otherwise). If these precautions were not obeyed a disordered structure with similar elements of structure resulted. Some of the presented STM images[18] are recorded in differential mode. Due to the inherent drift in STM at variable temperatures, the error in image size is on the order of 5%. Dosing of CO and Xe was performed at $T=20-190$ K by backfilling the chamber to $P=1\times10^{-9}-2\times10^{-8}$ mbar. The exposure is given in MLE [MLE = monolayer equivalent, 1 MLE corresponds to the surface atomic density of Pt(111), i.e., 1.50×10^{19} particles/m^2].

Figure 1(a) shows the ordered superstructure (appearing as a lattice of depressions) observed after water adsorption at $T_{ads}=140$ K (see Ref. 19 for large scale topographs). The water layer has an apparent height of (1.4 ± 0.1) Å [measured with respect to the uncovered Pt(111) surface still visible for submonolayer coverage] which varies smoothly with tunneling voltage (from 1.3–2.4 Å). For a clean tip it shows no contrast inversion, comp Ref. 20. The Fourier transform of the superstructure displays 12 peaks due to two rotational

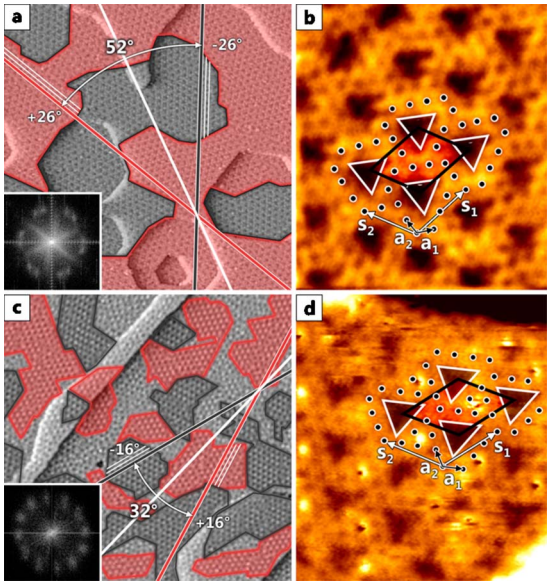

FIG. 1. (Color online) (a) STM topograph of the H_2O wetting layer on Pt(111) formed by adsorption at 140 K ($\sqrt{37}\times\sqrt{37}R25.3°$). The superstructure is characterized by a lattice of depressions spaced by 17 Å. Shading in false colors (dark, light) indicates two rotational domains (domain boundaries marked by black and light lines). The lines in the respective shadings are parallel to rows of depressions in the appropriate domain (also indicated by parallel thin lines). The angle bisector (white line) is parallel to the step edges of Pt vacancy islands, i.e., parallel to the dense packed $\langle 1\bar{1}0\rangle$ direction. The inset shows the respective Fourier transform. (b) Molecularly resolved STM image of the $\sqrt{37}$ with the supercell marked by a rhombus and associated supercell vectors $\mathbf{s}_1,\mathbf{s}_2$. Triangular depressions are marked by white triangles and lattice points associated with the dark spots are indicated by black dots. Primitive translations of the lattice partly populated by the dark spots are $\mathbf{a}_1$ and $\mathbf{a}_2$. (c) STM topograph of the H_2O wetting layer on Pt(111) formed by adsorption at 130 K ($\sqrt{39}\times\sqrt{39}R16.1°$). The superstructure is characterized by a lattice of depressions and additional protrusions. Color coding, construction of lines, and inset as in (a). (d) Molecularly resolved STM image of the $\sqrt{39}$ showing a periodic second layer decoration (white spots). Markings as in (b). Image parameters: width 710 Å [(a) and (c)], 81 Å (b), 68 Å (d), $U=0.5$ V [(a)–(c)], $U=0.2$ V (d), $I=60$ pA (a), $I=100$ pA (b), $I=160$ pA (c), $I=300$ pA (d), and width of the Fourier transforms in the insets of (a) and (c) 1.26 $Å^{-1}$.

domains of the hexagonal superstructure. The angle $\alpha=(52\pm2)°$ between rotational domains and the periodicity of (17.1 ± 0.9) Å ($a_{\sqrt{37}}=16.9$ Å) indicate that we observe the $\sqrt{37}\times\sqrt{37}R25.3°$ superstructure in real space [equivalent matrix notation $M_{\sqrt{37},\mathrm{Pt}(111)}=(7\ 4,\ -4\ 3)$ with respect to the substrate, see also Fig. 4]. In Fig. 1(b), the molecular structure of the $\sqrt{37}$ is resolved. The triangular depressions have an apparent depth between 0.6 and 1.0 Å with a mean value of (0.7 ± 0.1) Å, the error mainly given by the varying sharpness of the tip. They are separated by ridges containing dark spots. The dark spots are part of a hexagonal lattice with primitive translations $\mathbf{a}_1,\mathbf{a}_2$. The dense-packed rows of this lattice enclose an angle $\beta=5°$ with the ones of Pt(111). With respect to $\mathbf{a}_1$ and $\mathbf{a}_2$ the superstructure has a matrix

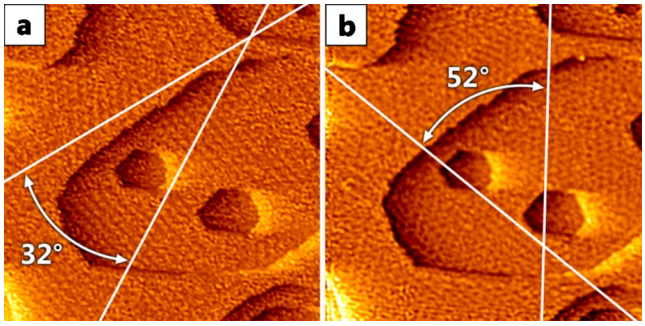

FIG. 2. (Color online) Phase transition from (a) $T=138$ K, $\sqrt{39}\times\sqrt{39}R16.1°$ symmetry to (b) $T=140$ K, $\sqrt{37}\times\sqrt{37}R25.3°$ symmetry within 8 min. The white dots vanish, enabling the water layer to reorganize as indicated by the change of the orientation of the superstructure. Image width 820 Å, $U=0.5$V, and $I=160$ pA.

$M_{\sqrt{37},H_2O}=(4\ 2,\ -2\ 2)$. We interpret the dark spots as centers of hexagonal ice rings. The structural model proposed in Ref. 11 does not comply with these observations.

For lower $T_{\mathrm{ads}}=130$ K, a second superstructure forms with prominent protrusions [Fig. 1(b)]. The Fourier transform shows two rotational domains with $\alpha=(32\pm2)°$. The measured periodicity is (18.0 ± 0.5) Å. We identify this structure with the second HOC superstructure: $\sqrt{39}\times\sqrt{39}R16.1°$ ($a_{\sqrt{39}}=17.3$ Å) or $M_{\sqrt{39},\mathrm{Pt}(111)}=(7\ 5,\ -5\ 2)$. Figure 1(d) shows that also the $\sqrt{39}$ builds from an ordered arrangement of triangular shaped depressions but with additional small bright protrusions imaged on the ridges with an apparent height above the water layer of (0.9 ± 0.1) Å (i.e., 70% of the water layer height under comparable tunneling conditions) and an average diameter of (5.5 ± 0.6) Å. For the superstructure we derive $M_{\sqrt{39},H_2O}=(4\ 3,\ -3\ 1)$ with $\beta=2°$. We could also prepare islands of the $\sqrt{37}$ at 130 K by adsorbing only 0.55 molecules per site.

The proposed arrangement of the H_2O lattice (forming the ridges) with respect to the substrate is backed by the evaluation of the spot intensities found in previous diffraction studies.[5,11,12] The spots with the highest intensities coincide with the reciprocal-lattice points calculated from the partly populated black dot lattice in our model. Note that this is not the case for the structure proposed originally[11] (for more details see Ref. 19).

The $\sqrt{37}$ and $\sqrt{39}$ can be reversibly transformed into each other through adsorption or desorption of molecules. One direction of this transformation can be induced by heating the $\sqrt{39}$ to 140 K. In Fig. 2 the angle between two rotational domains changes from $\alpha=(32\pm2)°$ to $\alpha=(52\pm2)°$ by heating. Simultaneously, the protrusions of the $\sqrt{39}$ disappear. Together these observations indicate that the $\sqrt{39}$ has a higher density than the $\sqrt{37}$. Once the $\sqrt{37}$ is formed, it is preserved upon cooling. The wetting layer can only be retransformed from the $\sqrt{37}$ to the $\sqrt{39}$ by subsequent exposure at 130 K.[19] The reversible transformations indicate that both are equilibrium phases of the wetting layer on Pt(111). The higher thermal stability of the $\sqrt{37}$ implies a higher binding-energy per molecule. Moreover, the fact that we never prepared the $\sqrt{39}$ without protrusions shows that they are an integral part of the $\sqrt{39}$.

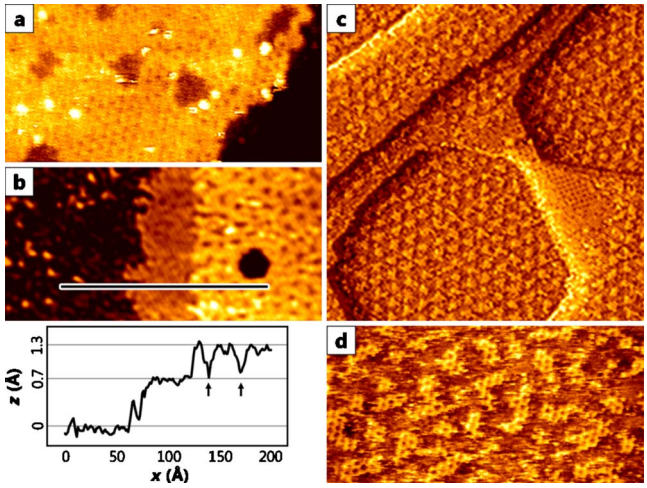

FIG. 3. (Color online) (a) STM topograph of the water layer after scanning with $U=-5$ V. A $\sqrt{3}$ structure is visible as well as patches of bare Pt. (b) STM topograph next to an area, where the water layer was removed by prolonged scanning at $U=-5$ V. In this transition region the Pt substrate, the dissociated and the intact water layer can be distinguished (see also the respective profile indicated by the black line, black arrows mark the depressions in the water layer). (c) STM topograph in inverted contrast imaging mode (see text) of the water layer after exposure to 1 MLE CO. The triangular depressions are now imaged as triangular protrusions rotated by 30°. (d) With the triangular protrusions as nuclei the $\sqrt{3}$ grows by prolonged scanning in the inverted contrast mode. Image parameters: width 140 Å (a), 320 Å (b), 310 Å (c), 180 Å (d), $U=0.3$ V (a), $U=0.5$ V [(b), (c), and (d)], $I=220$ pA (a), $I=190$ pA (b), and $I=150$ pA [(c) and (d)].

The wetting layer can be modified by prolonged scanning with $|U| \geq 4$ V as shown in Fig. 3(a). As the structure of this modified layer gives important clues on the structure of the intact layer, we will describe the effect of the prologued scanning in more detail. First a $\sqrt{3}$ structure results, as typical for $H_2O/Pt(111)$ after electron irradiation, usually explained by electron-induced partial dissociation of H_2O.[5,14] STM-induced dissociation is also known from related systems.[21] Continued scanning leads to the complete removal of the water layer from the surface. At the edge of water-free areas [Fig. 3(b)] a transition from the Pt surface (left) via the dissociated $\sqrt{3}$ (middle) to the $\sqrt{37}$ (right) can be observed. Three associated height levels can be determined in the respective line profile. For $U=0.5$ V, the dissociated phase has a height of (0.7 ± 0.1) Å, whereas the $\sqrt{37}$ has a height of (1.4 ± 0.1) Å. In literature, the established model for the equilibrium structure of a 1:1 mixed $(\sqrt{3} \times \sqrt{3})R30°$ OH $+H_2O$ structure is composed out of OH and H_2O in the same height above the substrate and with their molecular planes oriented parallel to the surface, i.e., a flat-lying geometry.[22] As we find the $\sqrt{3}$ motif and a comparably low apparent height after dissociation we interpret the structure observed in Fig. 3(a) as this flat-lying phase. A distinct $\sqrt{3}$ pattern was also observed after adsorption of H_2O under impure conditions. Here, the structure is imaged with the same apparent height as the surrounding wetting layer, in contrast to the structure described above. Note that the bottom of the triangular depressions in the intact water layer has approximately the same height as the $\sqrt{3}$ structure.

In the following we analyze the nature of the depressions as the common structural element of both the $\sqrt{37}$ and the $\sqrt{39}$. Several examples of an inhomogeneous appearance of an H_2O wetting layer have been reported. In Refs. 7 and 13 the structure was interpreted as a moiré pattern, i.e., an interference pattern arising when two similar grids are superimposed. However, this effect can be ruled out here as it cannot explain the different appearance of neighboring depressions, the rather large depth, or the sharp edges of these pits. Another possible explanation for the depressions are molecular vacancy clusters, similar to the lace structure reported for submonolayer coverages of H_2O on Pd(111),[10] which indeed bears a striking resemblance to the structures observed here. Geometrically, in such a flat hexagonal structure an imbalance between hydrogen bond donors and acceptors arises which leads to the appearance of holes in the water film.

It is reported that about 5% of the saturation coverage of CO adsorbs to the $\sqrt{39}$ and only a two-layer-thick ice film has a zero sticking probability for CO.[14] Does this observation corroborate the hole model? We tested this by dosing CO on a closed water layer. However, the appearance of the triangular depressions did not change even upon exposure in excess of 1 MLE CO. Instead, widely spaced islands of the CO $\sqrt{3} \times \sqrt{3}$ or $c(4 \times 2)$ structure[23] appeared inside the water layer [visible in Fig. 3(c) right from the center] indicating that CO is able to partly break up the H_2O layer here. Also for Xe no change in the appearance of the triangular depressions was observed.

During the CO experiments occasionally an inverted contrast STM imaging mode was encountered. We tentatively attribute this imaging mode to a CO molecule adsorbed to the PtIr tip. In inverted contrast mode the triangular depressions are imaged as protrusions with their triangular envelope rotated by 30°. The other parts of the wetting layer and CO islands are imaged 0.8 Å lower than the protrusions. Prolonged scanning in the inverted contrast mode causes the triangular protrusions in the wetting layer to grow to a connected pattern of the $\sqrt{3}$ [Fig. 3(d)], which displays the same height as the original protrusions. Apparently, the triangular protrusions are nuclei of the $\sqrt{3}$.

Based on the experimental results we suggest the following elements for the $\sqrt{37}$ and $\sqrt{39}$ as shown in Fig. 4. (i) The ridges of the superstructures consist of a hexagonal network of ice molecules derived from the lattice generated by the primitive translations $\mathbf{a}_1$ and $\mathbf{a}_2$ in Fig. 1. Each lattice point visible as a dark spot in Figs. 1(b) and 1(d) is surrounded by an ice ring. Consistent with previous results the ridges of the intact wetting layer are assumed to consist of a structure according to the H-down model.[4–7] Previous work rules out that a significant number of dangling hydrogen bonds points into the vacuum, which makes the first water layer hydrophobic, exemplified by three-dimensional ice growth on top. Consequently, we propose that the molecules in the ridges are arranged similar to the H-down model. However, as the position of the hydrogen atoms cannot be determined using STM we made no attempt to propose an orientation of individual water molecules shown in Fig. 4. Furthermore, we

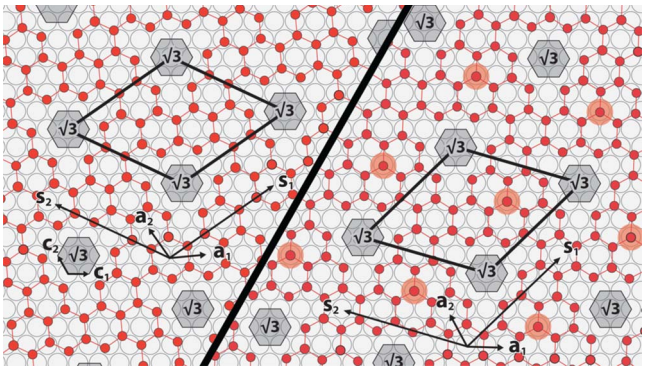

FIG. 4. (Color online) Sketches of the molecular structure (dismissing hydrogen atoms). Left: $\sqrt{37}\times\sqrt{37}R25.3°$ supercell. The ridge phase (circles) is an ice sheet in the H-down geometry whereas the depressions are segments of a $\sqrt{3}$ structure. The unit-cell vectors of the Pt $(\mathbf{c}_1,\mathbf{c}_2)$, the H_2O lattice $(\mathbf{a}_1,\mathbf{a}_2)$, and the superstructure $(\mathbf{s}_1,\mathbf{s}_2)$ are indicated. Right: model of the $\sqrt{39}\times\sqrt{39}R16.1°$ supercell. Symbols as in (a), in regions where the second-layer admolecules are found are marked by light circles.

made no attempt to relax the molecular positions. In the resulting $\sqrt{37}$ ($\sqrt{39}$), the hydrogen bond length of the molecules in the ridges is extended only by 0.7% (1.8%) compared to the one in bulk ice even if one neglects possible relaxations through the presence of the depressions. (ii) The triangular depressions are filled with water molecules forming the basic building block of the $\sqrt{3}$ or something very similar (gray hexagons in Fig. 4). As the triangular depressions are not empty, have under regular imaging conditions the same height as the $\sqrt{3}$ and act as their nuclei they are most probably filled with flat-lying molecules and/or flat-lying fragments in an $\sqrt{3}$ geometry. It has to be noted that a small flat-lying segment does not have to contain dissociated H_2O in order to avoid the occurrence of frustrated hydrogen bonds. If a complete hexagon of a nondissociated $\sqrt{3}$ phase is placed inside the depression one arrives at the structures recently proposed in Ref. 16. (iii) In addition, to the $\sqrt{39}$ in each unit-cell water in the second layer is adsorbed, thereby saturating dangling bonds, and thus lowering the energy.[24] This provides a simple explanation for the bright protrusions observed in Fig. 1(d). We assume that the protrusions are formed by a single water molecule, as we infrequently observe protrusions consisting of two or three dots which are most probably composed out of two or three water molecules.

In order to obtain a coverage estimate, we assume the same molecular density in the triangular depressions as in the ridge phase, leading to 0.65 (0.70) molecules/site for $\sqrt{37}$ ($\sqrt{39}$), in fair agreement with uptake measurements[25] for the $\sqrt{39}$. The ease of the phase transformation can be rationalized by the similarity of the two structures, the almost identical length of the OH bonds and the similar orientation of the dense-packed molecular rows. Note that the $\sqrt{37}$ is most probably identical to phase II in Ref. 13 whereas phase I from this reference could not be reproduced.

The authors acknowledge critical reading of the manuscript and technical advice by G. Pirug as well as discussions with P. J. Feibelman and the receipt of a preliminary DFT calculation. Also, the receipt of Ref. 16 is acknowledged. This study was financially supported by Deutsche Forschungsgemeinschaft.

*standop@ph2.uni-koeln.de

[1] P. J. Feibelman, Phys. Today **63**(2), 34 (2010).
[2] M. A. Henderson, Surf. Sci. Rep. **46**, 1 (2002).
[3] A. Hodgson and S. Haq, Surf. Sci. Rep. **64**, 381 (2009).
[4] H. Ogasawara, B. Brena, D. Nordlund, M. Nyberg, A. Pelmenschikov, L. G. M. Pettersson, and A. Nilsson, Phys. Rev. Lett. **89**, 276102 (2002).
[5] S. Haq, J. Harnett, and A. Hodgson, Surf. Sci. **505**, 171 (2002).
[6] N. G. Petrik and G. A. Kimmel, J. Chem. Phys. **123**, 054702 (2005).
[7] K. Thürmer and N. C. Bartelt, Phys. Rev. B **77**, 195425 (2008).
[8] S. Haq, C. Clay, G. R. Darling, G. Zimbitas, and A. Hodgson, Phys. Rev. B **73**, 115414 (2006).
[9] J. Carrasco *et al.*, Nature Mater. **8**, 427 (2009).
[10] J. Cerdá, A. Michaelides, M.-L. Bocquet, P. J. Feibelman, T. Mitsui, M. Rose, E. Fomin, and M. Salmeron, Phys. Rev. Lett. **93**, 116101 (2004).
[11] A. Glebov, A. P. Graham, A. Menzel, and J. P. Toennies, J. Chem. Phys. **106**, 9382 (1997).
[12] G. Zimbitas, S. Haq, and A. Hodgson, J. Chem. Phys. **123**, 174701 (2005).
[13] M. Morgenstern, J. Müller, T. Michely, and G. Comsa, Z. Phys. Chem. **198**, 43 (1997).
[14] J. Harnett, S. Haq, and A. Hodgson, Surf. Sci. **528**, 15 (2003).
[15] P. J. Feibelman, Phys. Rev. Lett. **91**, 059601 (2003).
[16] S. Nie, P. J. Feibelman, N. C. Bartelt, and K. Thürmer, Phys. Rev. Lett. **105**, 026102 (2010).
[17] A. Picolin *et al.*, J. Phys. Chem. C **113**, 691 (2009).
[18] I. Horcas *et al.*, Rev. Sci. Instrum. **78**, 013705 (2007).
[19] See supplementary material at http://link.aps.org/supplemental/10.1103/PhysRevB.82.161412 for further experimental results regarding the phase transformation and a detailed comparison of our model with the scattering data of Refs. 5, 11, and 12.
[20] K. Morgenstern and J. Nieminen, J. Chem. Phys. **120**, 10786 (2004).
[21] M. Mehlhorn, H. Gawronski, and K. Morgenstern, Phys. Rev. Lett. **101**, 196101 (2008).
[22] A. Michaelides and P. Hu, J. Chem. Phys. **114**, 513 (2001).
[23] G. Ertl, M. Neumann, and K. M. Streit, Surf. Sci. **64**, 393 (1977).
[24] G. Zimbitas, M. E. Gallagher, G. R. Darling, and A. Hodgson, J. Chem. Phys. **128**, 074701 (2008).
[25] C. Clay, S. Haq, and A. Hodgson, Phys. Rev. Lett. **92**, 046102 (2004).